A compact antenna design for UWB MIMO applications

Diseño de una antena compacta para aplicaciones UWB MIMO

María del Carmen Hernández-Serrano, Alin Denis Carbajal-Gasca and Luis Alejandro Iturri-Hinojosa[1]
ESIME-Zacatenco, Instituto Politécnico Nacional, Edif. 5, 1er. Piso, Col. Lindavista C.P. 07738, CDMX, México

Abstract. A compact UWB-MIMO antenna design with an impedance bandwith from 3.2 GHz to 9.1 GHz is presented. The MIMO antenna has a transmission coefficient response less than -14 dB at the resonance frequency bandwidth. To improve the isolation and the antenna performance, an Electromagnetic Band Gap (EBG) structure is introduced between elements, that consists of an added microstrip at ground plane, a 9x1 periodic metal-square patches on top of the substrate, and vertical vias connecting the patches to the ground plane. The EBG structure design methodology is presented. The isolation enhancement between elements is 4 dB at frequency bandwidth. The compact UWB-MIMO antenna with EBG structure reaches a maximum isolation of -33 dB at 6.42 GHz. The peak gain is 4.8 dBi at 7.3 GHz in the H-plane radiation, and 3.3 dBi at 7.3 GHz in the E-plane radiation.

Keywords. UWB; MIMO antenna; 2x1 compact antenna; EBG.

Resumen. Se presenta el diseño de una antena UWB-MIMO compacta 2x1 con un ancho de banda desde 3,2 GHz a 9,1 GHz. La antena MIMO tiene una respuesta de coeficiente de transmisión inferior a -14 dB en el ancho de banda de frecuencia de resonancia. Para mejorar el aislamiento y el rendimiento de la antena, se introduce una estructura de brecha de banda electromagnética (EBG) entre los elementos, que consta de una microcinta añadida en el plano de tierra, parches cuadrados de metal periódicos de 9x1 en la parte superior del sustrato y alambres verticales que conectan los parches al plano de tierra. Se presenta la metodología de diseño de la estructura EBG. La mejora del aislamiento entre elementos es de 4 dB en el ancho de banda de frecuencia. La antena compacta UWB-MIMO con estructura EBG alcanza un aislamiento máximo de -33 dB a 6,42 GHz. La ganancia máxima es de 4,8 dBi a 7,3 GHz en la radiación del plano H y de 3,3 dBi a 7,3 GHz en la radiación del plano E.

Palabras Claves. UWB; antenna MIMO; antenna compacta 2x1; EBG

How to Cite. . Hernández-Serrano, A. Carbajal-Gasca, and A. Iturri-Hinojosa, "A compact antenna design for UWB MIMO applications", *Jou. Cie. Ing.,* vol. 14, no. 1, pp. 39-49, 2022. doi:10.46571/JCI.2022.1.5

Received: 21/03/2022 **Revised:** 5/06/2022 **Accepted:** 30/06/2022

[1] *Corresponding author: aiturri@ipn.mx*

1. Introduction

In the last years, the demand for wireless communication systems has focused on information capacity, the greater rate in wireless communication, higher bandwidth, and compact antenna geometry. Also, the simultaneous requirement is increasing with the different wireless network technologies [1]. The Multiple-Input Multiple-Output (MIMO) technology is a good option to satisfy these demands. MIMO technology takes advantage of RF multipath coverage to increase the reliability and predictability of the wireless signal, resulting in higher throughput. These characteristics make it an essential technique for multiple technologies like Wireless Local Area Network (WLAN, 5.15-5.825 GHz), Worldwide Interoperability for Microwave Access (WiMAX, 3.3-3.6 GHz), Ultra-WideBand (UWB, 3.1-10.6 GHz), downlink of X-band satellite (7.25-7.75 GHz), Long Term Evolution (LTE), 5G, among others [1, 2, 3]. UWB antennas are characterized by a high transmission rate more than 100 Mbps, low power and multipath communications, maximum bandwidth utilization, their compact size, low profile, low fabrication cost, omnidirectional and bidirectional radiation pattern, and ultra-wide impedance bandwidth [2, 4]. Modern medical sciences are an important application for UWB MIMO antennas. This is where compact antenna arrays are required for monitoring systems to achieve high resolution and precise results for the detection of different stages of cancer [5].

The MIMO technology has outstanding advantages on the performance of wireless communication systems, like the capacity enhancement and the performance of the received and transmitted signals. The challenge for the designers is the conditioning in reduced spaces, proper user terminals and base stations. Due to the proximity of the antenna elements, the radiated energy can couple each other due to electromagnetic interactions. Intrinsic parameters of the antenna are modified, like terminal impedances and reflection coefficients. This mutual coupling between elements degrades radiation characteristics and the system performance significantly, for instance, decreases the signal to interference ratio (SINR) of an adaptative array, the array algorithms convergence and radar cross section (RCS) [3], [6], [7].

Several solutions have been proposed to reduce mutual coupling between the elements such as Electromagnetic Band Gap (EBG) structures [7]-[9], parasitic element slots [11], [12], defected ground structures (DGS) [13]-[15], and perforated ground planes.

In [16] a dual-polarized MIMO antenna integrated with EBG structure is presented. The EBG structure consists of periodical cells of dielectric elements. The bandwidth of the proposed antenna is from 5.70 to 5.93 GHz, reaches a peak gain of 5.45 dBi, with a maximum isolation of -20 dB.

UWB-MIMO system that consists of two 90° angularly separated semi-circular stepped monopoles with decoupling network is proposed in [17]. The antenna geometry is based on UWB circular monopole antenna. The antenna has two implementations; a uniplanar EBG structures and mushroom EBG structures to obtain triple notches in WiMAX, WLAN and X-Band satellite downlink communication. The simulated isolation magnitude of the proposed antenna throughout the band is greater than 15 dB.

The MIMO antenna proposed in [18] has two radiation patches with an EBG structure between elements and a rectangular-shaped ground plane etched on both sides of the antenna. The effect of the EBG structure is a reduction of the mutual coupling up to -30 dB, in the frequency band from 2.2 to 3.6 GHz and from 5.5 to 5.9 GHz.

[19] presents the design of a 10x1 MIMO antenna with a peak gain of 17.8dBi. The antenna reaches an impedance bandwidth of 4.1 GHz, and the array antenna area is 88mm × 9.8 mm, much wider than the MIMO antenna described in this paper.

A double-sided MIMO antenna with a decoupling structure for UWB applications is presented in [20]. The MIMO antenna with four square elements achieves a large bandwidth of 7.7 GHz from 3.3 GHz to 11 GHz, with an average gain of 4.36 dBi. Each element has similar shape to the square patch element of the MIMO antenna present here.

This paper exhibits the implementation of an EBG structure in a 2x1 MIMO antenna array, located between the two microstrip elements. The simulation of the MIMO antenna is performed with the help of the Ansoft HFSS software. The geometry of the EBG structure was optimized to reduce the mutual coupling between the elements and therefore enhance the performance application.

2. Rectangular Patch Antenna Design

The microstrip-line feed antenna is printed on FR4 epoxy dielectric substrate with a 4.4 dielectric constant (ε_r), thickness of 1.6 mm (h), loss tangent of 0.02 and is initially designed for the resonant frequency of 7 GHz.

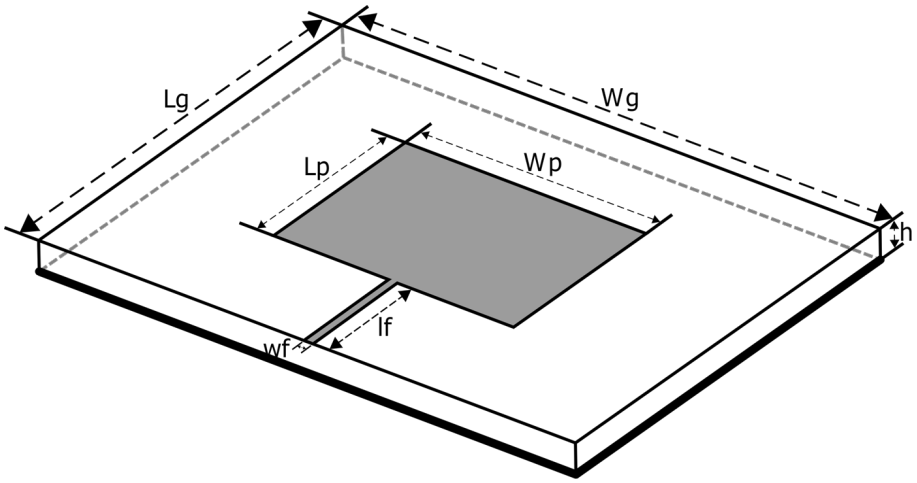

Figure 1: Microstrip antenna geometry.

The patch has a length L_p and a width W_p, and is printed over the dielectric substrate. The width and length of the ground plane are W_g ($=W+10h$) and L_g ($=Lp+2*Lf$), respectively, and is printed on the other side of the substrate. Analytical expressions used for the rectangular microstrip line feed design is presented in [21]. Fig. 1 shows the rectangular microstrip geometry.

The patch width W_p is given by:

$$W = \frac{\lambda_o}{2}\sqrt{\frac{2}{\varepsilon_r + 1}} \tag{1}$$

where $\lambda_o(\lambda_o = c/f)$ is the operating signal wavelength.

The effective dielectric constant is obtained with Eq. (2).

$$\varepsilon_{\varepsilon ff} = \frac{\varepsilon_r + 1}{2} + \frac{\varepsilon_r - 1}{2}\left(\frac{1}{\sqrt{1 + \frac{10h}{W}}}\right) \tag{2}$$

The incremental length (ΔL) for fringing field can be calculated with Eq. (3).

$$\Delta L = 0.412h\left[\frac{\varepsilon_{eff} + 0.3}{\varepsilon_{eff} - 0.258}\right]\left[\frac{\frac{W}{h} + 0.264}{\frac{W}{h} + 0.813}\right] \tag{3}$$

For the TM_{010} dominant mode without radiation fringes, considering the wavelength in the substrate (λ_g), the patch length (L) is equal to $\frac{\lambda_g}{2}$, where $\lambda_g = \frac{\lambda_o}{\sqrt{\varepsilon_{eff}}}$.

By considering the radiation fringes the patch length is given by

$$L = \frac{\lambda_g}{2} - 2\Delta L \tag{4}$$

The effective length of the patch is calculated with Eq. (5).

$$L_{eff} = L + 2\Delta L \tag{5}$$

The resonant frequency (f_r) of the antenna element is calculated using Eq. (6).

$$f_r = \frac{1}{2\sqrt{\mu_0\varepsilon_0}L_{eff}\sqrt{\varepsilon_{ef}}} \tag{6}$$

where μ_0 and ε_0 are the vacuum permeability and permittivity.

The patch antenna has an orthogonal radiation respect to the ground plane. The radiated electric field pattern is obtained using Eq. (7) to (9) [14].

$$E_\varphi^t = +j\frac{k_0 hwE_0 e^{-jk_o r}}{\pi r}\left\{sin\theta\frac{sin(X)}{x}\frac{sin(Z)}{z}\right\}\cdot cos\left(\frac{k_0 L_e}{2}sin\theta sin\varphi\right) \tag{7}$$

$$X = \frac{k_0 h}{2}sin\theta cos\varphi \tag{8}$$

$$Z = \frac{k_0 W}{2}cos\theta \tag{9}$$

The line feed is characterized by a length (l_f), a width (w_f) and a Z_f impedance and connect the patch with the SMA connector that has a Z_2 (=50 Ω) impedance. The patch impedance is calculated with Eq. (10).

$$Z_p = \frac{90\varepsilon_r^2}{\varepsilon_r - 1}\left(\frac{L}{W}\right)^2 \tag{10}$$

The line feed impedance is calculated with Eq. (11).

$$Z_f = \sqrt{Z_p Z_2} \tag{11}$$

The line feed length (l_f) in millimeters is calculated with Eq. (12).

$$l_f = \frac{\theta_{a,rad}}{k_0\sqrt{e}} \tag{12}$$

where $\theta_{a,rad}(=\pi/2)$ is the length of the coupling transmission line of quarter wavelength ($\lambda/4$) and e is calculated with Eq. (13).

$$e = 0.5(\varepsilon_r + 1) + \frac{0.5(\varepsilon_r - 1)}{\sqrt{1 + 12\frac{h}{W_0}}} \tag{13}$$

where $W_0 = W_d \cdot h$, for which $W_d = W_{d1}$ if $W_{d1} < 2$, either $W_d = W_{d2}$ if $W_{d1} \geq 2$. And

$$W_{d1} = \frac{8e^A}{e^{2A} - 2} \tag{14}$$

$$W_{d2} = \frac{2}{\pi}\left[B - 1 - In(2 * B - 1) + \frac{\frac{\varepsilon_r - 1}{2}}{\varepsilon_r} * \left(In(B - 1) + 0.39 - \frac{0.61}{\varepsilon_r}\right)\right] \tag{15}$$

With:

$$A = \frac{Z_0}{60} * \sqrt{0.5 * (\varepsilon_r + 1)} + \frac{\varepsilon_r - 1}{\varepsilon_r + 1}\left(0.23 + \frac{0.11}{\varepsilon_r}\right) \tag{16}$$

$$B = 377 * \frac{\pi}{2 * Z_0 * \sqrt{\varepsilon_r}} \tag{17}$$

With the above equations, the geometric parameters for the inset-feed patch antenna at 7 GHz are given in Table 1. The wavelength is equal to 42.85 mm, the effective dielectric constant (ε_{eff}) results equal to 3.781, the incremental length (ΔL) is 0.716 mm, the patch impedance (Z_p) and the line feed impedance (Z_f) are equal to 276.91 Ω and 117.67 Ω, respectively. In the antenna element, the ground plane size (w_g, l_g) is the same of the dielectric substrate.

Table 1: Geometric parameters of the patch antenna element.

Parameter	Value, mm
W_p	13.041
L_p	9.586
W_s	29.041
L_s	22.056
l_f	6.235
w_f	0.435

3. Patch Antenna Element

Some geometric dimensions were optimized to achieve a compact antenna geometry and a larger operating bandwidth. The performance optimization consists in increasing the patch size, width (W_p) and large (L_p), the dielectric substrate width (W_g), the line feeder width (W_f) in multiples of 0.1mm. At the same time, the ground plane has been reduced to 0.0λ and increased in multiples of 0.1mm until a minimum return loss response is achieved at the resonant frequency of 7GHz. Fig. (2) shows the rectangular patch antenna with optimized dimensions.

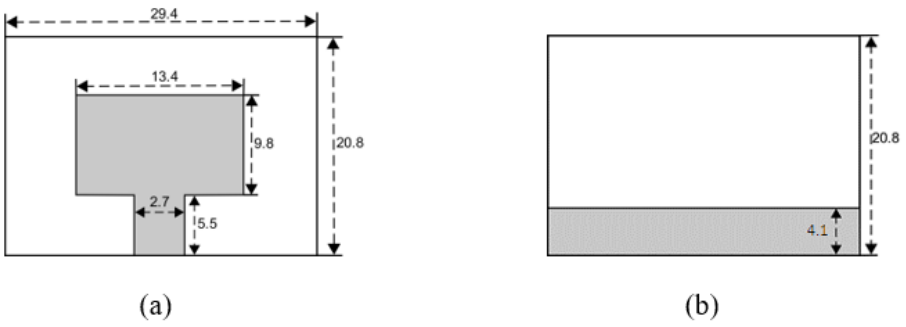

Figure 2: Patch antenna geometry (a) front and (b) back view. Units in millimetres.

A full-wave simulation of the proposed antenna is conducted with ANSYS High Frequency Structural Simulator (HFSS).

Fig. (3) presents the return loss response for different sizes of the ground plane (l_g), keeping its width (w_g) equal to that of the dielectric substrate. A 4.1 mm is considered as the adequate length of the ground plane to achieve the highest operating bandwidth and a peak gain equal to 2.38 dB in the H-plane radiation, and 0 dB in the E-plane radiation. Fig. (4) shows the return

loss comparison of the patch antenna with non-optimized dimensions from Table 1 with that of the patch antenna with optimized dimensions of Fig. (2).

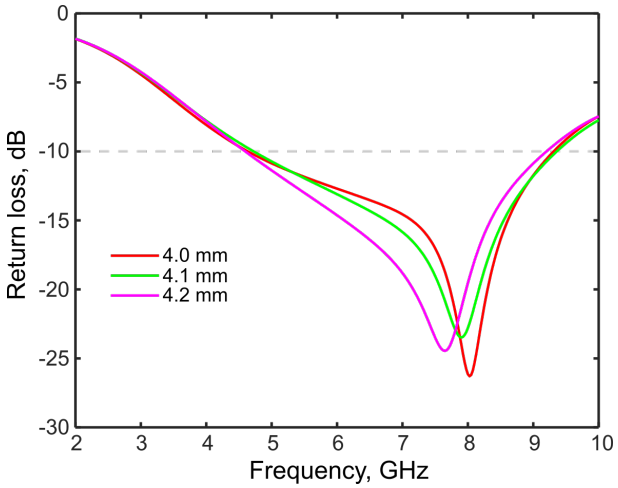

Figure 3: Simulated return loss for different lengths of ground plane.

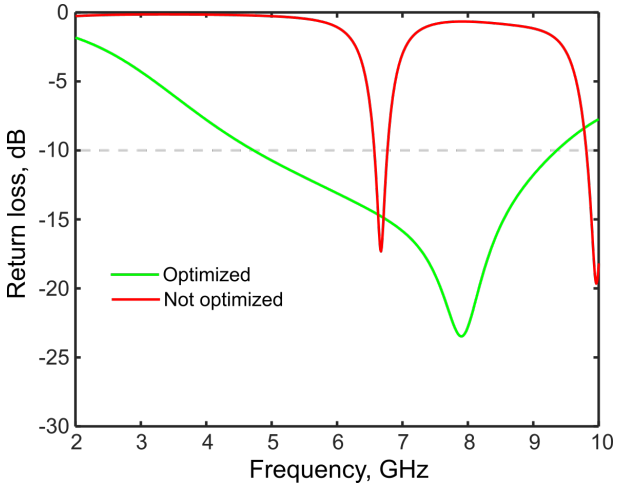

Figure 4: Simulated return loss for the optimized geometry.

The optimized patch antenna has an operating frequency band of 4.63 GHz, from 4.72 GHz to 9.35 GHz. The resonance frequency of the antenna is equal to 7.9 GHz, with a return loss value of -23.5 dB and a maximum gain of 2.38 dB.

4. The 2X1 MIMO Antenna

Two rectangular patch antennas of Fig. (2) are placed side to side, spaced 4 millimeters, to conform the MIMO antenna. The compact 2x1 MIMO antenna is 7.904 cm^2 ($3.8cm \times 2.08cm$). The antenna geometry with dimensions is shown in Fig. (5).

Simulated results of reflection (S_{11}) and transmission (S_{21}) coefficients are presented in Fig. (6). The operating bandwidth is 4.8 GHz, from 3.8 GHz to 8.6 GHz. A resonant frequency is observed at 5.6 GHz with reflection coefficients of -23 dB.

There is a strong electromagnetic coupling between the radiating patches since the transmission coefficient (S_{21}) is greater than -16 dB at the operation bandwidth.

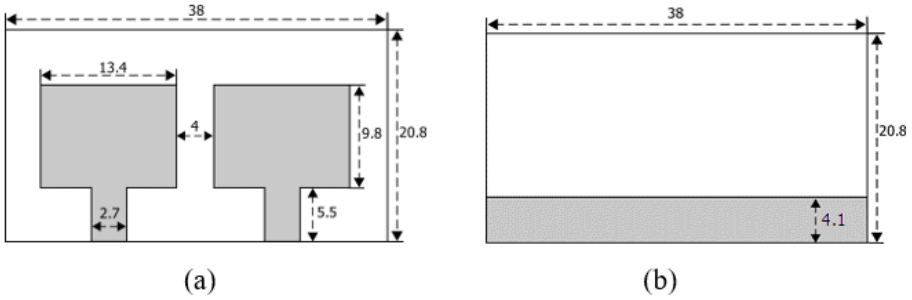

Figure 5: Geometry of the compact 2x1 MIMO antenna, (a) top and (b) back view. Units in millimeters.

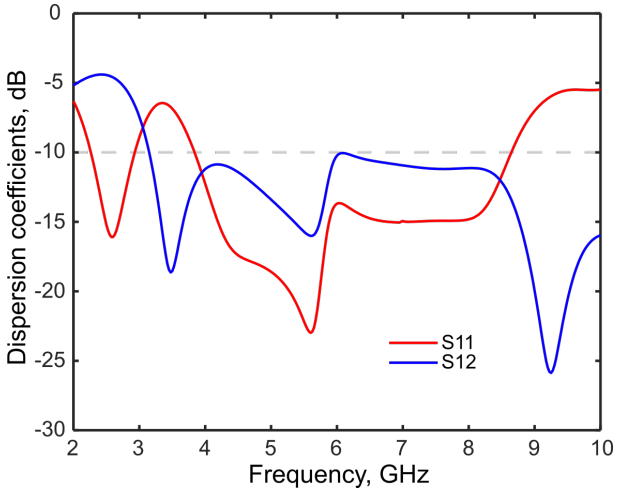

Figure 6: S parameters of the 2x1 MIMO array antenna.

5. The MIMO Antenna with EBG Structure

Good isolation between closely spaced antennas is required for MIMO communication systems. To improve the isolation, an Electromagnetic Band Gap (EBG) structure is designed and introduced between the antenna elements. Below, the methodology used for the design of the EBG structure is presented. The design of the EBG structure begins by adding a vertical microstrip of width w_v in the center of the ground plane. Fig. (7) presents the reflection and transmission coefficient responses of the MIMO antenna with 3 widths of the added microstrip. The geometry of the MIMO antenna that achieves the greatest bandwidth is the one with the 1mm wide vertical microstrip.

To the above MIMO antenna is added a row of 9x1 vertical square microstrips connected to each other by a microstrip of width 1.0 mm. Each square patch element has a side dimension a. Fig. (8) presents the return loss response of MIMO antennas with values of 1.5, 1.75 and 2.0 millimeters for the dimension a. The MIMO antenna with the widthest bandwidth is the one with $1.5mm \times 1.5mm$ square microstrips as the EBG structure. The transmission coefficient is below -15dB in the operating bandwidth.

To the 9x1 periodic metal patches ($1.5mm \times 1.5mm$) on top of the substrate connected with a 1mm width microstrip are added vertical viases connecting the square patches to the ground plane. The purpose of connected the decoupling structure to the ground is to neutralize the surface current and increase the gain of the antenna [15].

The compact 2x1 MIMO antenna dimension with EBG structure is 38 mm x 20.8 mm and

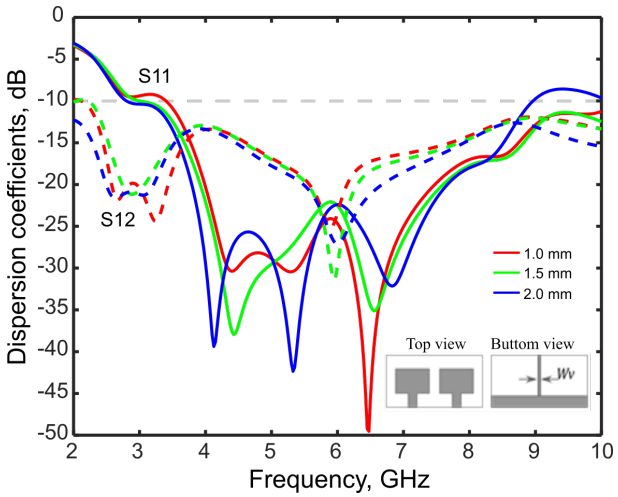

Figure 7: MIMO antena with a vertical microstrip in ground plane with different widths w_v.

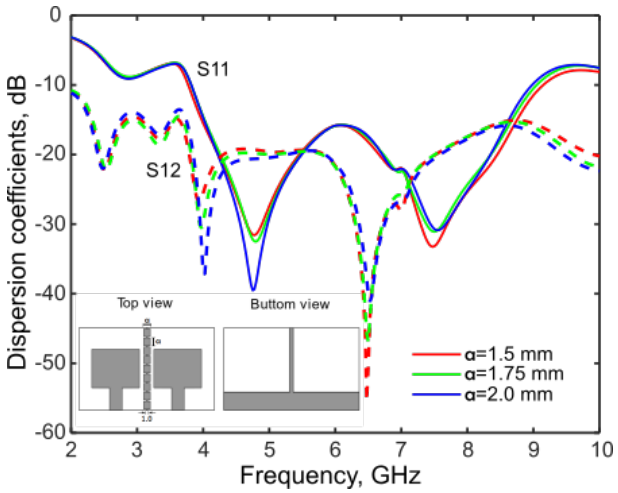

Figure 8: Dispersion coefficients for MIMO antenas with square patches connected with different microstrip widths.

is given in Fig. (9). The MIMO antenna with the EBG structure has a transmission coefficient of -41 dB and -29 dB at 4.325 GHz and 7.3 GHz, respectively. The operating bandwidth is 5.9 GHz, from 3.2 to 9.1 GHz.

The reflection (S_{11}) and transmission ($S_{12} = S_{21}$) coefficients obtained by simulation are shown in Fig. (10).

Fig. (11) shows the simulated far-field radiation patterns of the proposed UWB-MIMO antenna for E-plane and H-plane at the two operating bandwidths. In the E-plane radiation the maximum gains are 3.3 dB ($\theta = 235°$) and 0 dB ($\theta = 275°$) at the frequencies 7.3 GHz and 4.325 GHz, respectively. In the H-plane radiation the maximum gains are 4.8 dB ($\phi = 155°$) and 2.7 dB ($\phi = 117°$) at the frequencies 7.3 GHz and 4.325 GHz, respectively.

6. Conclusions

A 2x1 compact UWB-MIMO antenna design for 3.2 GHz to 9.1 GHz is presented. The MIMO antenna geometry is $7.904cm^2$ ($3.8cm \times 2.08cm$) and is conformed by two rectangular patches,

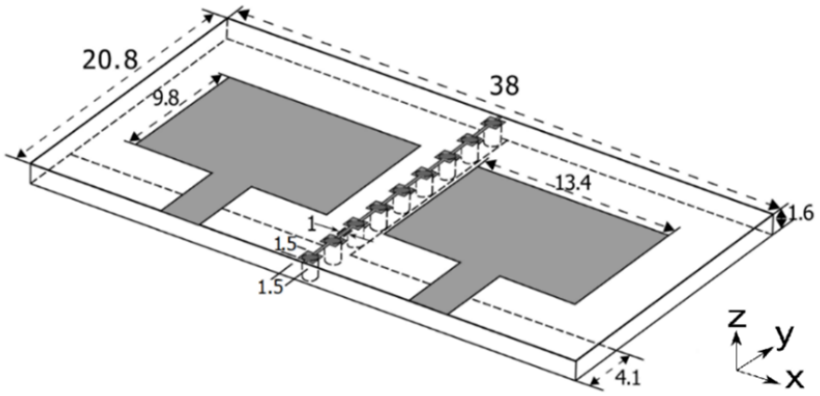

Figure 9: The compact 2x1 MIMO antenna with EBG structure. Units in millimeters.

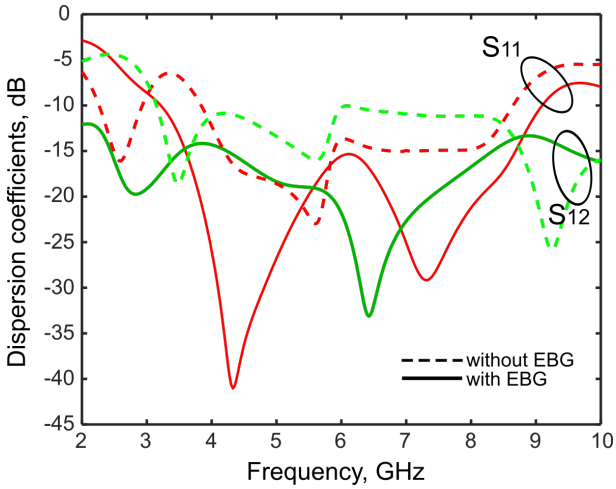

Figure 10: S parameters of the MIMO antenna with and without the EBG structure.

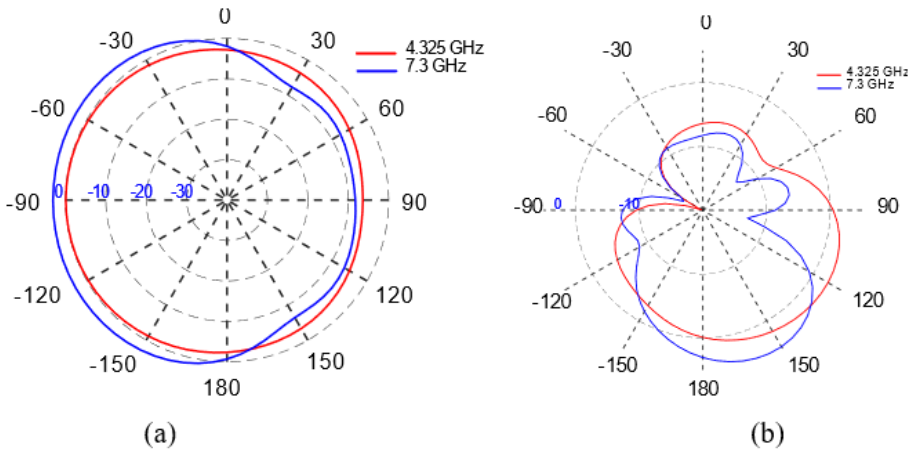

Figure 11: Normalized (a) E-plane ($\phi = 0°$) and (b) H-plane ($\theta = 90°$) radiation patterns of the proposed MIMO antenna.

each one with a resonance frequency at 7.9 GHz, a 4.6 GHz bandwidth, and a maximum gain of 2.38 dBi. An EBG structure is introduced between the elements to increase de isolation and improve the MIMO antenna performance. The transmission coefficient of the MIMO antenna with EBG structure reaches a minimum of -33 dB at 6.42 GHz, and its maximum is -13.3 dB at 8.85 GHz. The impedance bandwidth is 5.9 GHz, and the maximum gain of the proposed antenna is 4.8 dBi. Simulated results of S-parameters and radiation patterns are presented.

Acknowledgements
The authors express thanks to the support received by the project SIP20221930.

References

[1] Feng, Botao, et al. "A dual-wideband and high gain magneto-electric dipole antenna and its 3D MIMO system with metasurface for 5G/WiMAX/WLAN/X-band applications," *IEEE Access*, vol. 6, July 2018, pp. 33387-33398, doi: 10.1109/ACCESS.2018.2848476.

[2] Chen, Xiaoming, Shuai Zhang, and Qinlong Li. "A review of mutual coupling in MIMO systems." *Ieee Access*,vol. 6, May 2018, pp. 24706-24719, doi: 10.1109/ACCESS.2018.2830653.

[3] El Ouahabi, Mohssine, et al. "Analysis and design of a compact ultra-wideband antenna with WLAN and X-band satellite notch," *International Journal of Electrical and Computer Engineering*, vol. 10, no. 4, 2020, pp. 4261-4269, doi: 10.11591/ijece.v10i4.pp4261-4269.

[4] Daghari, Marwa, and Hedi Sakli."Radiation performance enhancement of an ultra wide band antenna using metamaterial band-pass filter," *International Journal of Electrical & Computer Engineering (2088-8708)*, Vol. 10, No. 6, Dec. 2020, pp. 5861 5870, doi: 10.11591/ijece.v10i6.pp5861-5870.

[5] Shaikh, Faraz Ahmed, et al. "Design and parametric evaluation of UWB antenna for array arrangement," *Bulletin of Electrical Engineering and Informatics*, vol. 8, no. 2, June 2019, pp. 644-652. doi: https://doi.org/10.11591/eei.v8i2.1522.

[6] Singh, Hema, H. L. Sneha, and R. M. Jha. "Mutual coupling in phased arrays: A review," *International Journal of Antennas and Propagation*, vol. 2013, DOI: http://dx.doi.org/10.1155/2013/348123.

[7] Abdelhamid, C., Sakli, H., & Sakli, N., "A four-element UWB MIMO antenna using SRRs for application in satellite communications," *International Journal of Electrical & Computer Engineering*, vol. 11, no. 4, pp. 2088-8708, Aug. 2021, doi: 10.11591/ijece.v11i4.pp3154-3167.

[8] Liu Li, Cheung SW, Yuk TI. "Compact MIMO antenna for portable devices in UWB applications" *IEEE Trans Antennas Propag.*, vol 61, no. 8, pp. 4257–64, Aug. 2013, doi: 10.1109/TAP.2013.2263277.

[9] Gallo Michele, Daviu EA, Bataller MF, Bozzetti Michele, Molina-Garcia-Pardo Jose Maria, Juan-Llacer Leandro. "A broadband pattern diversity annular slot antenna," *IEEE Trans Antennas Propag*, vol. 60, no. 3, pp. 1596-1600, Mar. 2012, doi: 10.1109/TAP.2011.2180314.

[10] F. Yang and Y. Rahmat-Samii, *Electromagnetic Band Gap Structures in Antenna Engineering*, 1st ed. Cambridge, U.K.: Cambridge Univ. Press, Oct. 2009, pp. 156-201.

[11] Mak Angus CK, Rowell Corbett R, Murch Ross D. "Isolation enhancement between two closely packed antennas," *IEEE Trans Antennas Propag*, vol. 56, no. 11, pp. 3411-9, Nov. 2008, doi: 10.1109/TAP.2008.2005460.

[12] Sun X-b, Cao M-y. "Mutual coupling reduction in an antenna array by using two parasitic microstrips," *Int J Electron Commun*, vol. 17, pp. 1-4, 2017, doi: 10.1016/j.aeue.2017.01.013

[13] Sharawi Mohammad S, Khan Muhammad U, Numan Ahmad B, Aloi Daniel N. "A CSRR loaded MIMO antenna system for ISM band operation," *IEEE Trans Antennas Propag*, vol. 61, no. 8, pp. 4265-4274, Aug. 2013, doi: 10.1109/TAP.2013.2263214.

[14] Zhu F-G, Xu J-D, Xu Q. "Reduction of mutual coupling between closely-packed antenna elements using defected ground structure," *Electron Lett*, vol. 45, no. 12, 2009, doi: 10.1109/MAPE.2009.5355659.

[15] Wei Kun, Li Jianying, Wang Ling, Xing Zijian, Rui Xu. "S-shaped periodic defected ground structures to reduce microstrip antenna array mutual coupling," *Electron Lett*, vol. 52, no. 15, pp. 1288-1290, July 2016, doi: 10.1049/el.2016.0667.

[16] Zhang, X. Y., Zhong, X., Li, B., & Yu, Y., "A dual-polarized MIMO antenna with EBG for 5.8 GHz WLAN application," *Progress In Electromagnetics Research*, vol. 51, pp. 15-20, 2015, doi: 10.2528/PIERL14112104.

[17] Jaglan, N., Gupta, S. D., Thakur, E., Kumar, D., Kanaujia, B. K., & Srivastava, S., "Triple band notched mushroom and uniplanar EBG structures based UWB MIMO/Diversity antenna with enhanced wide band isolation," *AEU-International Journal of Electronics and Communications*, vol. 90, pp. 36-44, 2018, doi: 10.1016/j.aeue.2018.04.009.

[18] Beigi, P., Rezvani, M., Zehforoosh, Y., Nourinia, J., & Heydarpanah, B., "A tiny EBG-based structure multiband MIMO antenna with high isolation for LTE/WLAN and C/X bands applications," *International Journal of RF and Microwave Computer-Aided Engineering*, vol. 30:e22104, 2020, doi: 10.1002/mmce.22104.

[19] Rahayu, Y., Sari, I. P., Ramadhan, D. I., & Ngah, R., "High gain 5G MIMO antenna for mobile base station," *International Journal of Electrical and Computer Engineering*, vol. 9, no. 1, Feb. 2019, pp. 468-476, doi: 10.11591/ijece.v9i1.pp468-476.

[20] Muhammad Aslam Hasin, M. T. Ali, Hamizan Yong, Bazilah Baharom, Hadi Jumaat, "Development of MIMO antenna with decoupling structure for ultra-wideband application,", *Indonesian Journal of Electrical Engineering and Computer Science*, vol. 16, no. 2, pp. 818, 2019.

[21] Balanis, C. A., *Antenna theory: analysis and design*, John wiley & sons, 2016, pp. 811-843.